

Quantitative NMR imaging of the short-T2 components in the SKM tissue: alterations observed in myopathic patients

Ericky Caldas de A. Araujo¹, Noura Azzabou¹, Alexandre Vignaud², Geneviève Guillot³, and Pierre G. Carlier^{1,4}

¹NMR Laboratory, Institute of Myology, Paris, Île-de-France, France, ²CEA/DSV/I2BM/NeuroSpin/UNIRIS, Gif Sur Yvette, Île-de-France, France,

³IR4M/UMR8081/CNRS, University Paris-SUD, Orsay, Île-de-France, France, ⁴NMR Laboratory, CEA/I2BM/MIRCen, Paris, Île-de-France, France

Target audience: Researchers interested on the application of new quantitative NMR methods in the field of neuromuscular disorders (NMDs).

Context: Muscle fibrosis is one of the main long term consequences of the chronic inflammatory/necrotic insults to skeletal muscle (SKM) in some NMDs. It starts as a progressive accumulation of collagen in the endomysium during the initial stages of the diseases, and there is general agreement that this abnormal increase of intramuscular connective tissue (IMCT) plays an important role promoting further progression of the disease. While the detection and quantification of inflammation and fatty infiltration are well accomplished with current quantitative NMRI methods [1], two main factors have hampered the NMRI of IMCT: (i) detection of NMR signals from protons in the collagen or in the water molecules hydrating these proteins using standard NMRI techniques is hampered by their short T2-values (~10 µs and ~1 ms respectively); (ii) imaging of endomysial layers using a *lack of signal* approach is hampered by the insufficient spatial resolution attainable with current NMRI techniques. Ultra-short Time to Echo (UTE) methods offer the possibility of acquiring signal at a very short delay after excitation (~100 µs), allowing one to acquire the NMR signal from protons in the hydration layers of the collagen. We have applied the UTE method for imaging the short-T2 signal in SKM tissue. Although different methods for separating the short- and long-T2 signals in UTE data exist [2], they fail when applied to SKM: long-T2 selective saturation methods are highly sensitive to B0 inhomogeneity and cannot provide saturation of the signal from all hydrogen groups in the lipids; image subtraction in dual-echo acquisition methods results in residual signal contributions from bulk water and lipids due to the T2*-decay of their signals and the complicated amplitude modulation of the NMR signal issued from lipids. In SKM, the short-T2 signal is a minority and can be easily biased by residual signal from the long-T2 components of water and lipids, hampering the access to any quantitative information. We propose a new method for processing UTE data, resulting in signal issued exclusively from the short-T2 components in the SKM, which we hypothesise to reveal IMCT content. The proposed method was applied to investigate the SKM tissue of healthy volunteers and patients diagnosed with NMDs.

Methods: Eight healthy volunteer and three patients underwent a protocol consisting on the acquisition of 7 images of the same axial slice placed at mid-length of the calf, at the echo times $TE = 0.2, 2.5, 3, 5, 7, 9.6$ and 26.5 ms using an UTE sequence. Examinations were performed on a 3 teslas (3T) whole-body scanner. Relevant sequence parameters were: $TR = 30$ ms, $FA = 5^\circ$, $BW = 357$ kHz, $FOV = 136 \times 136$ mm², *effective in-plane res.* = 0.34x0.34 mm², *slice thickness* = 6 mm, *Nb of radial lines* = 1024, *line res.* = 512. Total acquisition time per subject was 7 min 49 s. The following model was assumed for the signal evolution in each voxel: $S(TE) = (W_s e^{-TE/T_{2s}} + (W_l + F \times f(TE))e^{-TE/T_{2l}})e^{i\omega_0 TE}$. W_s and T_{2s} are real positive variables representing the amplitude at $TE = 0$ and the T2*-value characterizing the signal from the short-T2 components. W_l and F are real positive variables representing the amplitude at $TE = 0$ of the NMR signal issued from long-T2 components of water and from lipids, respectively, while T_{2l} represents the T2*-value characterizing their signals; $f(t) \equiv \sum_k \rho_k e^{i2\pi f_k t}$ is completely determined by the frequency spectrum that was assumed for the NMR signal from lipids, as described in [3]. ω_0 accounts for the offset frequencies due to B0 field inhomogeneities. Data processing consisted on two steps: (i) Determining the values of W_l , F and T_{2l} by application of a robust chemical-shift method [4] on the images acquired at $TE \geq 3$ ms, in which short-T2 signals are assumed to be negligible; (ii) Isolation of short-T2 signal by performing an algebraic operation with the images acquired at $TE_1 = 0.2$ and $TE_2 = 2.5$ ms, in which water and total fat magnetization vectors are assumed to be in-phase. The value of T_{2l} was used to demodulate both images and avoid residual signal from long-T2 components due to T2*-decay. As $f(t)$ is known a priori, the value F was used to subtract residual signal from lipids due to the intrinsic amplitude modulation of their signal. Distributions of the quantity $\hat{W}_s = W_s(e^{TE_1/T_{2l}} - e^{TE_2/T_{2l}} - e^{TE_1/T_{2s}} - e^{TE_2/T_{2s}})$, were obtained for each subject using the following operation: $|S(TE_1)|/e^{-TE_1/T_{2l}} - |S(TE_2)|/e^{-TE_2/T_{2l}} - F \times (|f(TE_1)| - |f(TE_2)|)$. Finally, maps of the relative fraction of the imaged signal, \hat{W}_s , were calculated as: $\frac{\hat{W}_s}{(\hat{W}_s + W_l + F)} \equiv \hat{W}_{s,frac}$.

Results: Figure 1 shows the maps of the relative fraction of short-T2 signal as obtained by different methods for a healthy volunteer: (a) simple subtraction; (b) demodulated subtraction; and (c) the proposed method ($\hat{W}_{s,frac}$). Figure 2 shows the extracted maps of $\hat{W}_{s,frac}$ and fat fraction for the three myopathic patients. Figure 3 presents the total histogram of the $\hat{W}_{s,frac}$ extracted in all subjects and the histograms of $\hat{W}_{s,frac}$ extracted in each of the three myopathic patients.

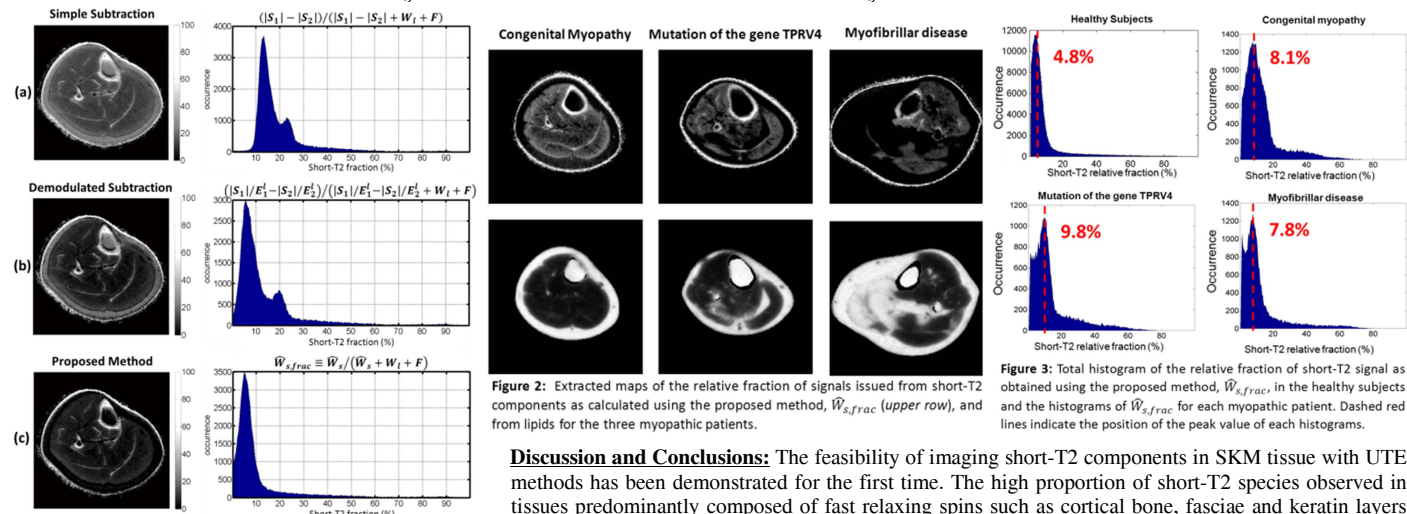


Figure 1 : Maps of the relative fraction of short-T2 signal, $\hat{W}_{s,frac}$, and corresponding histograms as calculated by different methods obtained for one healthy volunteer: (a) simple subtraction; (b) demodulated subtraction; and (c) the proposed method. The expression defining how the signal is calculated for each method is presented over the corresponding histogram.

Figure 2: Extracted maps of the relative fraction of signals issued from short-T2 components as calculated using the proposed method, $\hat{W}_{s,frac}$ (upper row), and the histograms of $\hat{W}_{s,frac}$ for each myopathic patient. Dashed red lines indicate the position of the peak value of each histograms.

Discussion and Conclusions: The feasibility of imaging short-T2 components in SKM tissue with UTE methods has been demonstrated for the first time. The high proportion of short-T2 species observed in tissues predominantly composed of fast relaxing spins such as cortical bone, fasciae and keratin layers of skin supports this contention. In tissues where the short-T2 components are a minority, such as SKM, long-T2* demodulation and subtraction of signal contributions from lipids are crucial for correctly isolating signal from short-T2 components (see Fig. 1). Our results suggest that the relative fraction of the imaged signal from short-T2 components is more important in patients with chronic neuromuscular diseases than in healthy subjects (Fig. 3). Although the high signal observed on fasciae drives us to hypothesise that the imaged signal in muscles shall come from the hydration water pools within the thinner collagen layers of the endomysium and perimysium, a fraction of the short-T2 component could also come from water molecules hydrating the intracellular proteins forming the contractile apparatus. Further investigations are necessary to determine the histological compartmentation of the imaged short-T2 components in SKM. On the future we shall apply this methodology on animal models to compare our results with histological analysis.

References: [1] Hollingsworth et al. 2012. Neuromusc. Dis. 22:S54-S67. [2] Du et al. 2011. Magn. Res. Imag. 29:470-482. [3] Azzabou et al. 2014. JMRI. [4] Hernando et al. 2010. MRM 63:79-90.